iHandRehab: An interactive hand exoskeleton for active and passive rehabilitation

Article *in* IEEE International Conference on Rehabilitation Robotics : [proceedings] · June 2011

DOI: 10.1109/ICORR.2011.5975387 · Source: PubMed

4 authors, including:

Jiting Li
Beihang University (BUAA)
21 PUBLICATIONS **292** CITATIONS
SEE PROFILE

Yuru Zhang
Beihang University (BUAA)
201 PUBLICATIONS **1,681** CITATIONS
SEE PROFILE

iHandRehab: an Interactive Hand Exoskeleton for Active and Passive Rehabilitation

Jiting Li*, Ruoyin Zheng, and Yuru Zhang
State Key Laboratory of Virtual Reality Technology and Systems
Beihang University
Beijing 100191, China
*lijiting@buaa.edu.cn

Jianchu Yao
Department of Engineering
College of Technology and Computer Science
East Carolina University
Greenville, NC U.S.A. 27858

***Abstract*—This paper presents an interactive exoskeleton device for hand rehabilitation, iHandRehab, which aims to satisfy the essential requirements for both active and passive rehabilitation motions. iHandRehab is comprised of exoskeletons for the thumb and index finger. These exoskeletons are driven by distant actuation modules through a cable/sheath transmission mechanism. The exoskeleton for each finger has 4 degrees of freedom (DOF), providing independent control for all finger joints. The joint motion is accomplished by a parallelogram mechanism so that the joints of the device and their corresponding finger joints have the same angular displacement when they rotate. Thanks to this design, the joint angles can be measured by sensors real time and high level motion control is therefore made very simple without the need of complicated kinematics. The paper also discusses important issues when the device is used by different patients, including its adjustable joint range of motion (ROM) and adjustable range of phalanx length (ROPL). Experimentally collected data show that the achieved ROM is close to that of a healthy hand and the ROPL covers the size of a typical hand, satisfying the size need of regular hand rehabilitation. In order to evaluate the performance when it works as a haptic device in active mode, the equivalent moment of inertia (MOI) of the device is calculated. The results prove that the device has low inertia which is critical in order to obtain good backdrivability. Experimental analysis shows that the influence of friction accounts for a large portion of the driving torque and warrants future investigation.**

Keywords-exoskeleton; thumb; index finger; rehabilitation; parallelogram mechanism; active and passive rehabilitation

I. INTRODUCTION

Hand plays a very crucial role in people's daily activities. However, it is often subjected to impairment: it may lose its motor function as results of accidents or diseases with the tender bones, muscles, and tendons. In order to recover the normal functions, hand rehabilitative training is needed.

Recently, issues associated with applying mechatronic devices and virtual reality technology into hand rehabilitation have attracted much research attention [1-13]. These hand rehabilitation devices realized various exercises. Some aimed at simple finger actions such as pinching, closing, and opening [2-4]. These rehabilitation devices usually have simple structure but can realize few DOFs. Many others devoted to providing broader exercises in order to train the finger manipulation ability [5-13]. This paper focuses on the latter.

Hand exoskeleton scheme has been widely investigated because of its complicated structure and design challenges [6-15]. Some of these devices were developed as force feedback devices [5][14][15], which can only apply force in a single direction, incapable of driving the finger bi-directionally. These devices can only be used in the active rehabilitative training mode. Others were designed as continuous passive motion machine [7] or works under the self-motion control mode [6]. Yet others can work in both active and passive modes, including the exoskeleton developed by Wege, *et al*. at the Technical University of Berlin [8]. This system has 4 DOFs and can actuate each finger joint by the means of a linkage mechanism. However, the system requires additional changeable attachments to fit different hand sizes. Worsnopp, *et al*. in Northwestern University [9] proposed a virtual prototype with 3 DOFs that was assembled on the lateral side of the finger. Yamaura, *et al.* presented a hand rehabilitation device [10] that can be adjusted to accommodate various hand sizes, but their device can achieve only two DOFs for each finger thus cannot train finger joints individually. The HANDEXOS system developed by Chiri, *et al*. [11] in Italy has three active rotational joints for flexion/extension, a passive rotational joint for abduction/adduction, and a passive translational joint for the kinematic coupling of the human/exoskeleton MP axes for each finger. The exoskeleton proposed by Wang [13] uses a double slider mechanism to realize the motion of flexion/extension of index finger joints. This mechanism, however, does not provide sufficient ROM because the slider stoke is limited by the length of finger phalanx.

Despite of these extensive research efforts, many issues involved in exoskeleton for hand rehabilitation remain still unresolved and challenging: none of these developed devices can simultaneously realize the following design goals often required by practical rehabilitation: adaptability to individual hand, changeability of the joint range of motion (ROM), suitability to the thumb, and realization of the DOFs needed to train each finger independently.

This paper presents iHandRehab, an interactive exoskeleton device for hand rehabilitation with features designed to achieve

The research is supported by National Natural Science Foundation of China (Grant No. 50975009).

these needs: 1) It can work in both passive and active modes; i.e., it can provide bi-directional movement for passive motion, and apply virtual feedback force to the finger as an interactive haptic device for active mode. 2) It can conduct rehabilitation exercises simultaneously for both the thumb and index finger. 3) Each finger has 4 DOFs so that all the finger joints can be trained independently. 4) The joint ROM and phalanx length are adjustable to accommodate different hand sizes.

The rest of the paper is arranged as follows: it starts with an overview of the proposed system in Section II, after which Section III elaborates the detailed mechanism design. Section IV studies several important issues about the applicability of the device and presents the experiment results, which lead to discussions before the conclusions of the paper.

II. Overview of the System

As shown in Fig. 1, the hand rehabilitation system is comprised of the hand exoskeleton integrated with angle and force sensors, the control system (including the controller and driver), and the virtual environment.

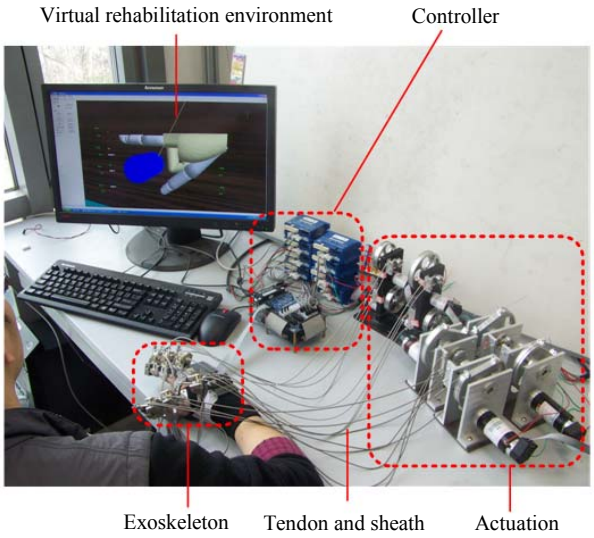

Figure 1. Prototype of the proposed exoskeleton.

The exoskeleton is worn on the dorsal side of the hand, which drives the human hand in passive motion, or follows the active motion of the hand. Details of the exoskeleton design are provided in the next section.

The control system samples the sensor data, sends the control commands to the motors, and communicates with the host computer with the TCP/IP protocol. The driver (Accelnet Micro Panel, Copley Inc, USA [16]) is set to run under the torque mode in human active motion. It can be digitally changed to the velocity mode in human passive motion.

The host computer runs the virtual rehabilitation environment (VRE) and the graphic user interface (GUI). The GUI allows a therapist to choose the rehabilitation motion mode and to set the rehabilitation training parameters, such as ROM, training time, and speed. The VRE simulates the rehabilitation exercises of the hand and provides the force feedback to the hand in active motion.

III. Design of the Device

A. Kinematic Model of the Thumb and Index Finger

As shown in Fig. 2, the thumb and index finger were modeled as two open chains. The index finger has four joints: the 1-DOF distal interphalangeal (DIP) and proximal interphalangeal (PIP) joints are parallel to each other; the 2-DOF metacarpalphalangeal (MCP) joint is modeled as two 1-DOF joints MCP1 and MCP2 with the right-angle intersectional rotational axes, where the MCP1 joint is assumed parallel to the DIP and PIP joints.

Likewise, the thumb has four joints, where the 1-DOF interphalangeal (IP) and metacarpalphalangeal (MCP) joints are parallel to each other; the 2-DOFs carpometacarpal (CMC) joint is modeled as two 1-DOF joints CMC1 and CMC2 with the right-angle intersectional rotational axes. Again, the CMC1 joint is parallel to the IP and MCP joints.

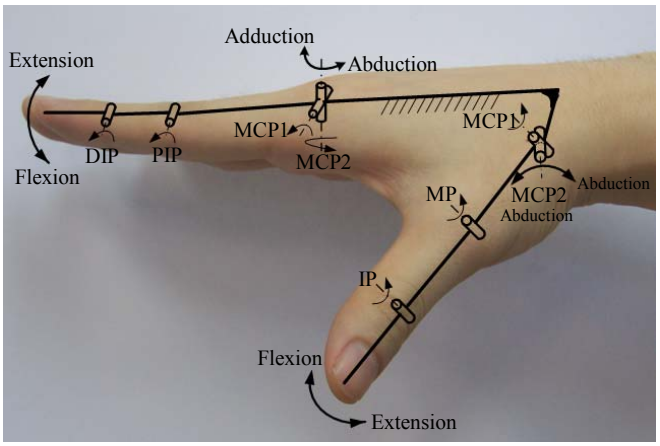

Figure 2. Kinematic model of the thumb and index finger.

B. Design of the Hand Exoskeleton

Based on the human hand model proposed above, the exoskeleton was designed as shown in Fig. 3.

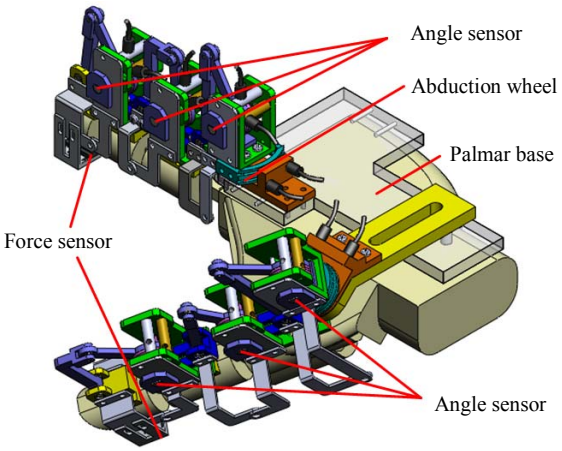

Figure 3. Virtual prototype of the exoskeleton.

The thumb and index finger modules are fixed on a palmar base at the locations determined by that of the human hand.

The palmar base, the thumb and index finger exoskeletons were mounted with Velcro on the dorsal side of the hand to prevent interference with the hand workspace.

Since the exoskeletons of thumb and index finger have the same structures, we use only the index finger as an example to explain the design details.

As introduced in the index finger model, the finger exoskeleton consists of four joint modules: DIP, PIP, MCP1 and MCP2, which respectively realize the flexion/extension of the DIP, PIP, and MCP1 joints, and abduction/adduction of the MCP2 joint. So the exoskeleton can realize all 4 DOFs of the index finger, as demonstrated in Fig. 3. The three flexion/extensions are realized by parallelogram mechanisms. The abduction/adduction of the MCP2 joint is realized by driving an abduction wheel. All the joints are supported with ball bearings and the material of most parts is aluminum. The entire hand exoskeleton weights approximately 250 grams.

The parallelogram mechanism proposed in Fig. 4 simplifies the relationship between the joint angles of the exoskeleton and human finger and therefore, makes the high level motion control more convenient. The parallelogram mechanism of the DIP joint module is described here; other parallelogram mechanisms are alike. In Fig. 4, link 7 is the relative fixed link; link 8 is the driving link, which is driven by the cable transmission; link 10 is fastened to the distal phalanx of the finger. Links 7, 8, 9, and 10 form the parallelogram mechanism. The rotating angle of link 10, $\Delta\theta$, which is also the rotating angle of the finger's DIP joint, is always equal to that of link 8, $\Delta\alpha$, which can be directly measured by the angle sensor installed on the fixed rotating shaft of link 8. Therefore, the control of the angle of the finger joint can be easily realized by rotating link 8 the same angle.

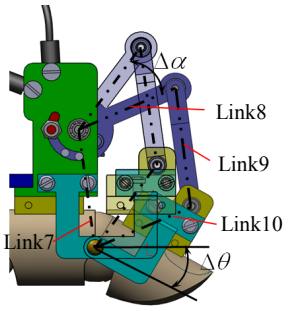

Figure 4. Paralellogram mechanism for each finger joint.

Accommodating hand size differences so that the device can be used for different patients is important. Different hand sizes generally imply different finger phalange lengths: the distance from the fingertip to DIP, from DIP to PIP, and from PIP to MCP1. When the exoskeleton is worn on the human hand, the joints J_{DIP}, J_{PIP} and J_{MCP1} of the exoskeleton need to be aligned with their finger joints, which means that the distance l_M and l_P are required to be adjustable (as shown in Fig. 5) to accommodate different hand sizes. In our design, the relative positions of adjacent exoskeleton modules are determined by a fastening screw, which can be moved in a slot on the connection slider before it is fastened.

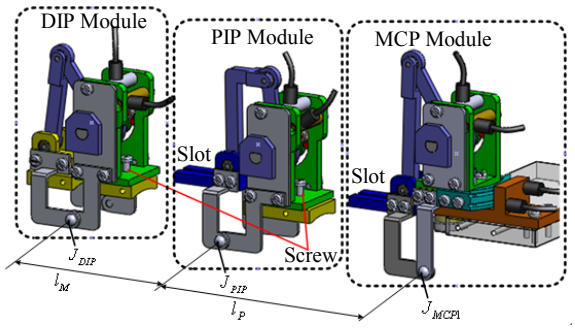

Figure 5. Adjustable connection between joint modules.

Design with safety in mind is critical for rehabilitation systems described here, because impaired hands are much more vulnerable than healthy hands due to the loss of sensation and motor ability. Safety design in the mechanical structure, combined with the safety features in the software and control levels, provides patients with multiple protections from re-hurting their hands. Different patients have different motor capabilities; even for the same patient, the ROM can gradually change during the process of motor function recovery. Thus, the maximum rotating angle should be restricted at an adjustable position. A mechanical structure was designed to meet this need. In the DIP module in Fig. 6, for example, a stop slider can slide along an arc slot that is coaxial with the rotation axis of the driving link. A stop pin fixed on and rotating together with the driving link can also move along the arc slot. The maximal angle between the stop pin and stop slider determines the allowed ROM. By fixing the stop slider at different positions of the arc slot, the ROM can be modified. So the safety mechanism can be adapted to different patients with different motor abilities.

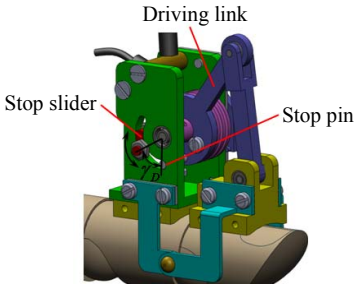

Figure 6. Mechanical stop

C. *Actuation and Transmission*

As shown in Fig. 1, the actuation module is located distantly from the hand in order to reduce weight imposed on the patient hand. A total of eight motors (RE25, RE36, Maxon Motor, Switzerland [17]) were fixed on the desktop frame to provide force and motion transmitted to the finger joints by a reducer and a cable/sheath transmission mechanism. Moreover, the cable/sheath transmission allows the hand to move in a relatively large space to accomplish rehabilitation exercises. To realize bi-directional movement, two cables were used for each joint motion. Considering the backdrivability required in active mode, the transmission ratio for each joint is designed less than

8. More details on actuation and transmission can be found in the authors' earlier work [13].

D. Sensors Integration

On each joint shaft, a potentiometer (SV01A103, MURATA manufacturing Co., Ltd, Japan [18]) was integrated to measure the rotational angle of the finger joint. Force sensors (Honeywell_FSS, USA [19]) were used to measure the force exerted by the human fingertips (shown in Fig. 3). Because the measuring area (a small spherical surface) of the sensors is too small for a soft fingertip to obtain reliable force measurement, three sensors were assembled together on the bottom of the distal module. The three sensors were covered with a thin metal plate as shown in Fig. 7 to ensure that the force exerted by the hand could be measured accurately. The output forces on the contact points of the three sensors were summed to obtain the resultant force exerted by the finger [20]. This output force was also used to compensate the resistant torque in active mode control [21].

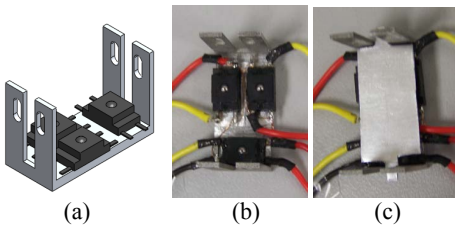

(a) (b) (c)

Figure 7. Force sensor assembly: (a) Overview; (b) Topview; (c) Sensors covered by a metal plate.

IV. Experimental Results and Discussion

A. Joint Range of Motion

In order to maximize the rehabilitation outcome, the ROM that an exoskeleton allows the finger to reach should be closely approximate to the natural ROM of a healthy finger. To assess this performance, the maximal joint angles were measured with and without the hand wearing the exoskeleton. Under both conditions, the subject rotated each joint to the maximum angle for three times. Ten healthy right-handed volunteers at the age of twenty to thirty (2 females and 8 males) participated in the experiment. For every joint, a total of thirty angle values were collected and the averages of the joints for the thumb and index finger are listed in Table I and Table II, respectively.

TABLE I. Maximum Joint Angles of the Thumb with and without Exoskeleton

Thumb	Joint (°)			
	IP	***MP***	***CMC1***	***CMC2***
With Exos.	71.0	78.0	33.4	28.4
Without Exos.	82.0	86.0	35.1	32.3
Difference	11.0	8.0	1.7	3.9

TABLE II. Maximum Joint Angles of the Index Finger with and without Exoskeleton

Index finger	Joint (°)			
	DIP	***PIP***	***MCP1***	***MCP2***
With Exos.	46.5	102.2	84.2	24.0
Without Exos.	65.0	119.7	92.0	24.0
Difference	18.5	17.5	7.8	0

The results in the tables show that the maximal angle of each joint with the device is smaller than that without. This is because the Velcro straps tightened the soft tissue of the phalange pads and thus constrained the motion of the joints to some extent. Besides, there might be some measurement errors caused by the rough fabrication. Nonetheless, these results are acceptable given that patients usually have less motor ability than healthy individuals and the slightly smaller limit angles serve a means of protection for the patient.

B. Range of Phalange Length

Tables III and IV compare the adjustable phalanx length range in our design to the statistics of phalanx lengths for disabled hands collected from about 250 samples [22][23]. From the statistic data, the average phalanx length of thumb is 28 mm, 35 mm, and 45 mm from distal to metacarpal; the corresponding average phalanx length of index finger is 17 mm, 25 mm, and 43 mm. It is obviously that the exoskeleton presented here covers the size of an average hand well and works for hands ranging from average to larger size.

TABLE III. Comparison of the Length of Phalange of the Thumb

Thumb	Phalange length (mm)		
	Distal	***Proximal***	***Metacarpal***
Statistics	18~36	28.6~57.2	22.3~44.7
Adjustable	⩾15	30~40	40~50

TABLE IV. Comparison of the Length of Phalange of the Index Finger

Index finger	Phalange length (mm)		
	Distal	***Middle***	***Proximal***
Statistics	11.1~22.1	16.3~32.6	27.9~55.9
Adjustable	⩾15	22~30	40~55

C. Moment of Inertia

In rehabilitation applications, when it moves actively, the finger experiences the moment of inertia (MOI) effect caused by the exoskeleton and actuation module. Small joint MOI is desired in order to obtain good backdrivability when the device is used in the active rehabilitation mode.

The equivalent MOI seen from the different phalanges is utilized to measure the effect on the finger. Since the same formulation applies to all joints, only details for the MCP1 joint module are given here, without losing universality.

Fig. 8 represents the schematic diagram of the exoskeleton, where the coordinate systems are set up in different modules according to the well-known D-H method [24].

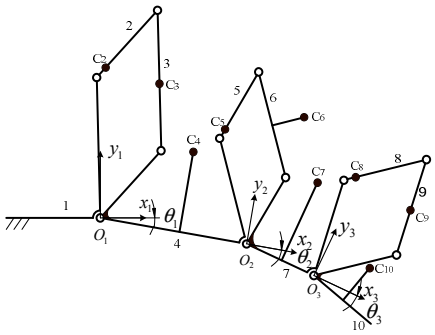

Figure 8. Kinematic sketch of the hand exoskeleton

Link 1 (fixed on the metacarpal phalange) is the relative fixed frame and link 4 is chosen to be the equivalent link. The equivalent MOI can be expressed as follows:

$$J_E = J_{Ee} + J_{Ea}, \tag{1}$$

where J_{Ee} and J_{Ea} represent the equivalent MOI of the exoskeleton and its actuation module, respectively.

The equivalent MOI of the exoskeleton is calculated in the following equation according to the principle of equivalency of kinetic energy.

$$J_{Ee} = \sum_{j=2}^{10}\left[m_j \left(\frac{v_{Cj}}{\omega_4} \right)^2 + J_j \left(\frac{\omega_j}{\omega_4} \right)^2 \right] \tag{2}$$

where v_{Cj}, ω_j, m_j, and J_j are the linear velocity of the center of mass, angular velocity, mass, and inertia of the *j*th link, respectively. Though the PIP and DIP joints were designed to be able to move independently, when the person moves the finger freely, the rotating angle of the DIP joint is coupled with that of the PIP joint with the following relationship [25].

$$\theta_3 = \frac{2}{3}\theta_2 \tag{3}$$

So their angular velocity relationship is obtained as follows.

$$\omega_{10} = \frac{2}{3}\omega_7 \tag{4}$$

Because the PIP and MCP1 joints move independently, the velocity ratios of links 5, 6, and 7 to link 4 are unknown. But we observed that some relationship may exist between movements of different joints when the patient moves the fingers. So we just take some ordinary motions to measure the velocity ratio aforementioned: for instance, the index finger takes the motion of flexion and extension at a regular speed. Four healthy subjects volunteered to participate in the experiment. They were asked to wear the exoskeleton and move their index finger freely. Meanwhile the angular velocities of the MCP1 and PIP joints were recorded by the angle sensors fixed on the exoskeleton. The results show that the angular velocities of the MCP1 and PIP joints are almost uniform. The result is modeled as follows.

$$\omega_4 = \omega_7 \tag{5}$$

From (2), (4) and (5), it is easy to know that J_{Ee} is the function of the rotating angle θ_1 of link 4.

The equivalent MOI of the actuation module can be calculated using the same method, the details of which are omitted here for simplicity.

In our design, the maximal equivalent MOI of the DIP, PIP, and MCP1 joints are $53.4 kgmm^2$, $95.8 kgmm^2$, and $217 kgmm^2$, respectively. These calculation results show that the designed exoskeleton has the low moment of inertia desired in the active rehabilitation mode.

D. Friction

Friction is another important factor that influences the backdrivability of an exoskeleton, which is much needed in active hand rehabilitation. In the presented design, the friction is mainly generated from the cables and cable sheathes. In spite that Kaneko investigated this kind of friction based on Coulomb's friction law [26] and indicated that the friction depends on many parameters, such us the curvature, pretension, length of the cable, etc, many difficulties prevent analytical friction analysis. The curvature, considered to be the constant in the model, actually changes during finger movement; the pretension is difficult to determine without the additional measurement instrument. It is impractical to calculate friction based on the model. Hence, we proposed an experimental method to directly estimate the resistant torque caused by the friction to provide a basis for succeeding work on friction compensation. We assumed that the quantity of friction torque between the cable and sheath is independent from the rotating direction as well as the motion mode.

Experiments were conducted in the following conditions. Each joint module was driven to rotate through the entire ROM by a constant motor toque while the other joints were fixed at the zero position (stretched straight relative to the preceding phalanges) so that there was no Coriolis force acted on the device and the centrifugal force generates zero torque. The hand was put at a position that the gravity is orthogonal to the flexion/extension plane so that the gravity does not generate torque on this plane either. The cable was kept as straight as possible to minimize the friction. The angular position was measured by the angle sensors during the rotating process, from which the angular acceleration can be calculated. Given the equivalent MOI seen from each joint (as described in the part C of section IV), we can get the friction torque produced by the friction.

Assuming that the exoskeleton is driven by the motor toque τ_k and the corresponding angular acceleration of joint is $\ddot{\theta}_k$, according to the equilibrium equation, we have

$$i_k \tau_k = (M_f)_k + (J_E)_k \ddot{\theta}_k \tag{6}$$

where $(M_f)_k$ is the friction torque produced by the friction and *k* denotes the joint module of DIP, PIP, and MCP1.

Equation (6) shows that a portion of the motor torque overcomes the friction torque, and the rest overcomes the equivalent MOI of the system. The percentage that the friction

torque accounts for the motor driving torque was calculated. Results are demonstrated in Fig. 9. It is found that the percentage of friction torque accounting for the driving torque is up to 95% during stable movements, which means that, in the proposed device, friction is the most significant factor that affects the backdrivability. Future investigation is necessary to explore methods that can reduce or compensate the friction.

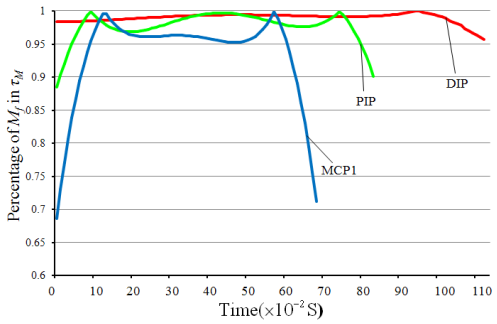

Figure 9. Results of friction experiment.

V. CONCLUSIONS

This paper introduced an exoskeleton device with a total of eight DOFs for thumb and index finger rehabilitation. The system designed here satisfies the requirements by both active and passive rehabilitaiton. The proposed device features lightwight, low inertia, capability of independent control of all finger joints, accommadation to different hand sizes with changeable ROM, and a mechanical safety design. All of these features bring great potential for its further rehabilitation appliations.

Experiment results from this research also show that friction between the cables and sheaths is the main factor that affects the backdrivability. Friction compensation will be investigated in the future.

REFERENCES

[1] H. C. Fischer, K. Stubblefield, K. Tiffany, X. Luo, R. V. Kenyon, and D. G. Kamper, "Hand rehabilitation following stroke: A pilot study of assisted finger extension training in a virtual environment," Topics in Stroke Rehabilitation, Jan.- Feb. 2007.

[2] Olivier Lambercy, Ludovic Dovat, Roger Gassert, Etienne Burdet, Chee Leong Teo, and Theodore Milner, "A Haptic Knob for Rehabilitation of Hand Function," IEEE Trans. on Neural Systems and Rehabilitaiton Engineering, 2007, vol. 15, no. 3, pp.356-366.

[3] U. Mali, and M. Munih, "HIFE-Haptic interface for finger exercise," IEEE/ASME Transactions on Mechatronics, 2006, vol. 11, no. 1. pp.93-102.

[4] L. Dovat, O. Lambercy, V. Johnson, B. Salman, S. Wong, R. Gassert, E. Burdet, T. C. Leong and T. Milneret, "A cable driven robotic system to train finger function after stroke," in Proc. 2007 IEEE 10th International Conf. Rehabilitation Robotics, Noordwijk, Netherlands, June 13-15, 2007, pp. 222-227.

[5] M. Bouzit, G. Burdea, G. Popescu, and R. Boian, "The Rutgers Master II – New design force–feedback glove," IEEE/ASME Trans. Mechatronics, 2002, vol. 7, no. 2, pp. 256-263.

[6] S. Ito, H. Kawasaki, Y. Ishigre, M. Natsume, T. Mouri, and Y. Nishimoto, "A design of fin motion assist equipment for disabled hand in robotic rehabilitation system," in Proc. First International Conf. Modeling, Simulation and Applied Optimization, Feb. 2005.

[7] Y. L. Fu, P. Wang, S. G. Wang, H. S. Liu, and F. X. Zhang, "Design and development of a portable exoskeleton based CPM machine for rehabilitation of hand injuries," in Proc. 2007 IEEE International Conf. Robotics and Biomimetics, Dec. 2007, pp. 1476-1481.

[8] A. Wege, K. Kondak, and G. Hommel, "Mechanical design and motion control of a hand exoskeleton for rehabilitation," in Proc. IEEE International Conf. Mechatronics and Automation, 2005, pp. 155-159.

[9] T. T. Worsnopp, M. A. Peshkin, J. E. Colgate, and D. G. Kamper, "An actuated finger exoskeleton for hand rehabilitation following stroke," in Proc. 2007 IEEE 10th International Conf. Rehabilitation Robotics, 2007, pp. 896-901.

[10] H. Yamaura, K. Matsushita, R. Kato, and H. Yokoi, "Development of hand rehabilitation system for paralysis patient – Universal design using wire-driven mechanism," in Proc. 31st Annual International Conf. IEEE EMBS, MN, USA, Sep. 2-6, 2009, pp. 7122-7125.

[11] A. Chiri, F. Giovacchini, N. Vitiello, E. Cattin, S. Roccella, F. Vecchi, and M.C. Carrozza, "HANDEXOS: towards an exoskeleton device for the rehabilitation of the hand," in Proc.The 2009 IEEE/RSJ International Conf. on Intelligent Robots and Systems,St. Louis, USA, October 11-15, 2009:1106-1111.

[12] T. Mouri, H. Kawasaki, Y. Nishimoto, T. Aoki, and Y. Ishigure, "Development of robot hand for therapist education/training on rehabilitation," in Proc. 2007 IEEE/RSJ International Conf. Intelligent Robots and Systems, San Diego, CA, USA, Oct. 29–Nov.2, 2007:2295-2300.

[13] J. Wang, J. Li, Y. Zhang, S. Wang, "Design of an exoskeleton for index finger rehabilitation," in Proc. 31st Annual International Conf. IEEE EMBS, Minneapolis, MN, USA, Sep. 2-6, 2009, pp. 5957-5960

[14] http://www.cyberglovesystems.com/products/cybergrasp/overview

[15] Mark J. Lelieveld, Takashi Maeno, and Tetsuo Tomiyama, "Design and Development of Two Concepts for a 4 DOF Portable Haptic Interface With Active and Passive Multi-Point Force Feedback for The Index Finger," in Proc. ASME 2006 International Design Engineering Technical Conference & Computers and Information in Engineering Conference, September 10-13, 2006, Philadelphia, Pennsylvania, USA.

[16] http://www.copleycontrols.com

[17] http://www.maxonmotor.com/

[18] http://www.murata.com/

[19] http://sensing.honeywell.com/

[20] Li Jiang, Mark R. Cutkosky, Juhani Ruutiainen, and Roope Raisamo, "Using Haptic Feedback to Improve Grasp Force Control in Multiple Sclerosis Patients," in IEEE Trans. on Robotics, vol. 25, no. 3, JUNE 2009, pp.593-601.

[21] Shuang Wang, Jiting Li, Ruoying Zheng, Zhongyuan Chen, and Yuru Zhang, "Multiple Rehabilitation Motion Control for Hand with an Exoskeleton", in Proc. 2011 IEEE intl. Conf. on Robotics and Automation, in press.

[22] Y.Y.Huang, and K.H.Low, "Initial Analysis and Design of an Assistive Rehabilitation Hand Device", 2008 IEEE International Conference on Systems, Man and Cybernetics(SMC 2008).pp.2586-2590.

[23] Robert Feeney, "Specific anthropometric and strength data for people with dexterity disability", Consumer and Competition Policy Directorate, Department of Trade and Industry, London,August 2002,pp.

[24] Z.X.Cai. *Robotics*.Qinghua University Press,2009.09

[25] Y. R. Zhang, J. T. Li, J. F. Li. *Robot dexterous hand: Modeling, Planning and Simulation*. China Machine Press,2007

[26] M Kaneko, M Wada, H Maekawa, K. Tanie. A new consideration on tendon-tension control system of robot hands. In Proc. 1991 IEEE International Conf. Robotics and Automation, Sacramento, CA, Apr. 1991: 1028-1033